Exhibit C

Martine Remy-Jardin, MD • Jacques Remy, MD • Charles Boulenguez, MD • Annie Sobaszek, MD
Jean-Louis Edme, MD • Daniel Furon, MD

Morphologic Effects of Cigarette Smoking on Airways and Pulmonary Parenchyma in Healthy Adult Volunteers: CT Evaluation and Correlation with Pulmonary Function Tests[1]

A prospective computed tomographic (CT) study was performed to determine the prevalence of lung changes in smokers. The study group comprised 175 healthy adult volunteers (current smokers, $n = 98$; ex-smokers, $n = 26$; nonsmokers, $n = 51$). The subjects underwent clinical examination, pulmonary function tests, chest radiography, and conventional and high-resolution CT (HRCT). Significant differences between current smokers, ex-smokers, and nonsmokers were observed with HRCT in the identification of subpleural ($P = .11$) and parenchymal ($P < .001$) micronodules, emphysema ($P < .001$), and areas of ground-glass attenuation ($P = .0001$). All subjects had normal pulmonary function. Parenchymal micronodules, areas of ground-glass attenuation, and emphysema were observed with a significant predominance in the upper lung zones ($P < .01$). Presence of emphysema and abnormal bronchial wall thickening were the only HRCT signs associated with significantly lower values of functional parameters. These data support the concept that parenchymal abnormalities can be detected in healthy smokers with normal findings at chest radiography and pulmonary function tests.

IF emphysematous changes and chronic inflammatory lesions of the bronchial tree are common consequences of chronic cigarette smoke exposure, there is abundant pathologic evidence supporting the notion that early changes occurring in the lungs of smokers are characterized by inflammatory changes in the lower respiratory tract (1–10). These changes consist of an accumulation of pigment-laden macrophages in respiratory bronchioles, the hallmark of small airways disease, and are usually observed with various degrees of bronchiolar inflammation and fibrosis. The latter is considered the most important feature responsible for abnormalities in small-airways function tests (5–7).

Small-airways inflammation is consistently associated with increased alveolar cellularity (mainly comprising pigment-laden macrophages) and interstitial anthracosis, the latter corresponding to deposition of free tobacco smoke particles or particles phagocytosed by macrophages within the interstitium. Although the most severe lung changes can be evaluated with clinical examination, pulmonary function tests, and chest radiography, there is general consensus that these examinations are of limited value in the assessment of early pathologic changes that are usually considered to be subclinical abnormalities.

The concept of an early and reversible stage of chronic obstructive pulmonary disease in healthy smokers and the ability of computed tomography (CT) to depict mild alterations in lung parenchyma have raised the hypothesis that lung lesions in smokers could be detected early with this technique. Our study was designed to assess lung changes in apparently healthy smokers on CT scans and to correlate them with results of pulmonary function tests.

MATERIALS AND METHODS

Subjects

From December 1989 to June 1991, we prospectively evaluated 230 healthy adult volunteers for whom a social, medical, and smoking history was available. These volunteers, all urban dwellers, were recruited from hospital workers in our institution and contacted at the time of their annual health-care evaluation by one physician (A.S.). The study was approved by the Hospital Ethics Committee, and written informed consent was obtained from all subjects before inclusion in the study.

Clinical evaluation was performed by means of a standardized questionnaire, modified from one used by the British Occupational Hygiene Society Committee on Hygiene Standards (11), and included questions about the presence of any isolated respiratory symptom (eg, cough, sputum production [both recorded as occurring in the morning or all day], dyspnea, and wheezing) or chronic bronchitis. Chronic bronchitis was diagnosed with the criteria defined by the American Thoracic Society (12); symptoms chiefly consisted of cough with sputum production and occurred for at least 3 months a year for at least 2 consecutive years. The severity of dyspnea was graded on a scale of 0 to 4, where grade 0 = no dyspnea; grade 1 = dyspnea occurring only after strenuous activity, such as climbing three flights of stairs, heavy housework, or walking more than 1 mile on level ground; grade 2 = dyspnea occurring with light housework or after climbing one flight of stairs; grade 3 = dyspnea occurring after minimal activity such as walking one or two

blocks on level ground; and grade 4 = dyspnea at rest or with eating or talking.

Subjects were included in the study on the basis of (a) knowledge of their medical background (eg, whether they had previously undergone chest surgery; whether they had pleural disease or previous respiratory illness, especially bronchiolitis of any origin in previous years or in infancy; and known exposure to environmental and/or occupational pollutants); (b) knowledge of their smoking history (quantitative estimates of the number of cigarettes consumed [number of pack-years] and duration of cigarette consumption [total life-time cigarette consumption]); and (c) absence of respiratory complaints. The latter criterion led to inclusion in the study group of subjects with a truly normal clinical evaluation or minimal respiratory symptoms, varying from isolated symptoms (cough, sputum production, or dyspnea after strenuous activity) to mild chronic bronchitis, that were only detected by means of the questionnaire and commonly considered as "normal" symptoms among smokers.

We systematically excluded subjects with severe dyspnea (grades 2 or 3) and all forms of chronic bronchitis complicated by respiratory infections and/or right ventricular failure. Subjects were also excluded from the final study group if evidence of extensive intrathoracic abnormalities (eg, parenchymal scars, infiltrates of unknown origin) was seen at CT or if they did not complete all the phases of the study. Our final study group comprised 175 subjects (115 women, 60 men) ranging in age from 20 to 55 years (mean plus or minus standard deviation, 33.4 years ± 6.87). The group was separated into current smokers (smoked regularly for more than 5 years; $n = 98$); ex-smokers (have not smoked for more than 2 years; $n = 26$), and nonsmokers ($n = 51$). Pulmonary function tests were performed immediately after clinical evaluation; chest radiographs (posteroanterior and lateral views) and CT scans were obtained within 3 weeks after inclusion in the study.

Pulmonary Function Tests

Pulmonary function tests were performed to obtain flow-volume curves. Maximum expiratory flow-volume curves were obtained by measuring flow with a pneumotachygraph (Spiroanalyser ST-300; Fukuda, Nagareyama, Japan). Calibration of the pneumotachygraph, maneuvers performed, and selection of curves met the American Thoracic Society guidelines (13,14). The following parameters were evaluated: forced vital capacity (FVC); forced expiratory volume in 1 second (FEV$_1$); ratio of FEV$_1$ to FVC; maximal expiratory flow (MEF); maximal expiratory flow at 75%, 50%, and 25% of FVC (MEF 75, MEF 50, MEF 25); maximal midexpiratory flow (MMEF); and midexpiratory flow at the end of expiration (MEF 25-15). Except for MEF 50/MEF, all spirometric values were expressed as a ratio of measured to predicted values. Prediction

equations were previously given by Knudson et al (15,16) for all parameters except MEF 25-15, which were obtained from Morris (17). Because of the technical limitations of the apparatus used in this protocol, diffusing capacity was not measured.

Chest Radiography

Posteroanterior and lateral chest radiographs were interpreted in random order by two chest radiologists (M.R.J., J.R.) independently of interpretation of the CT scans. The observers had no knowledge of the subject's smoking history, symptoms, or results of pulmonary function tests; final interpretation was obtained by consensus. Each radiograph was evaluated for the presence of a low-positioned diaphragm (defined as flattening of the diaphragm) and/or widened costophrenic angles (defined as rounded, rather than sharp, inferior margins of the lateral costophrenic angles), focal or diffuse oligemia, and bullae; emphysema was diagnosed if at least two of the above criteria were met. Presence of thickened bronchial walls, either seen on-end or as tram-line shadows, was also assessed. Interobserver agreement was calculated as the number of images on which the two observers agreed divided by the total number of images.

CT

Technique.—CT was performed with either an Elscint 2400 (Hackensack, NJ) or a Siemens Somatom Plus (Erlangen, Germany) unit. Both conventional and high-resolution CT (HRCT) were performed in the same imaging session. In the conventional CT study, 10-mm-thick scans were obtained at 15-mm intervals, extending from the lung apices to below the costophrenic angles, with a 350-mm field of view, a 512 × 512 reconstruction matrix, and either 130 kV and 315 mA (Elscint) or 137 kV and 145 mA (Siemens). Thick collimation images were reconstructed with a high-spatial-frequency algorithm for parenchymal analysis. HRCT was performed with a 1-mm section thickness at 15-mm intervals with a 512 × 512 reconstruction matrix, either 130 kV and 420 mA (Elscint) or 137 kV and 255 mA (Siemens), a 240-mm field of view, and a high-spatial-frequency algorithm.

HRCT was targeted to one lung to optimize the detection of fine parenchymal details; we chose to evaluate the right lung to reduce the adverse effects of cardiovascular motion artifacts, which can substantially compromise the overall quality of parenchymal analysis of the left lung. Both techniques were performed at the suspended end-inspiratory volume with a 1-second (Siemens) or 2-second (Elscint) scanning time, without intravenous administration of iodinated contrast material. All subjects were scanned in the supine position. Additional sections were obtained with the subjects in the prone position, when necessary, to demonstrate the reversibility of dependent areas of at-

tenuation. All images were obtained at window levels appropriate for lung parenchyma (conventional CT, 1,400 and −400 HU; HRCT, 1,700 and −600 HU).

CT scans were interpreted independently and in random order by each observer (J.R., M.R.J.), without knowledge of the subject's clinical history or smoking habits; the final interpretation was obtained by consensus. The interobserver agreement resulting from the independent analysis of conventional and HRCT scans (before final interpretation by consensus) was calculated as the number of images on which the observers agreed divided by the total number of images.

Analysis.—Our CT analysis was based on the hypothesis that morphologic changes in smokers' lungs could be detected with CT. Specific abnormalities evaluated included the following: (a) parenchymal and subpleural micronodules (<7 mm in diameter), which were expected to indicate the presence of respiratory bronchiolitis and subpleural interstitial anthracosis, respectively (size of nodular lesions was derived with previously reported criteria for CT analysis [18]); (b) areas of ground-glass attenuation (slightly hyperattenuating areas in which underlying vessels and bronchial walls remain visible, detected only on HRCT scans), which were expected to result from accumulation of inflammatory cells in the alveolar spaces (smoker's alveolitis); (c) dependent areas of attenuation in the posterior lung (these areas disappeared with the patient in the prone position; this CT sign was recorded in an attempt to evaluate the relationship between small-airways disease and the presence of dependent areas of attenuation); (d) emphysema, characterized as areas of decreased attenuation and disruption of the vascular pattern, usually lacking a well-defined wall (bullous emphysema was defined as regions of emphysema possessing a wall less than 1–2 mm thick; paraseptal emphysema was recorded as subpleural peripheral distribution of emphysema; each category of emphysema was coded separately); (e) bronchial abnormalities, including bronchial wall thickening (central bronchial thickening was diagnosed when the bronchial wall was at least twice as thick as that of normal bronchi; peripheral bronchial wall thickening was diagnosed with identification of peripheral bronchi with well-delineated bronchial walls), presence of bronchectases and bronchiolectases (bronchiolectases was recognized by abnormal visualization of bronchi in peripheral locations [dilated bronchiolar divisions seen along their length when horizontal or peripheral "signet ring" signs when coursing in a vertical direction]), and presence of abnormal bronchial content (mucoid impactions and/or bronchoceles); and (f) septal lines (thickened interlobular septa identified as fine linear areas of attenuation or as a polygonal pattern of multiple polygonal lines), expected to represent multiple interstitial anthracosis. In the evaluation of bronchial abnormalities, a separate analysis of the central

Table 1
Subject Characteristics

Parameter	Smokers (n = 98)	Ex-smokers (n = 26)	Nonsmokers (n = 51)
Age (y)*	33.0 ± 6.20	36.1 ± 7.38	32.7 ± 7.59
Height (cm)*	167.8 ± 7.86	168.2 ± 10.08	168.2 ± 8.28
Weight (kg)*	63.0 ± 11.43	66.6 ± 15.76	63.7 ± 10.20
Cigarette consumption (pack-years)*	12.8 ± 10.41	11.7 ± 7.03	...
Sex†			
Women	63 (64)	18 (69)	34 (67)
Men	35 (36)	8 (31)	17 (33)

* Data are given as mean ± standard deviation.
† Numbers in parentheses are percentages.

Table 2
Clinical Findings

Clinical Finding	Smokers (n = 98)	Ex-smokers (n = 26)	Nonsmokers (n = 51)	P Value*
Cough				
Morning	29 (30)	3 (12)	3 (6)	<.001
All day	13 (14)	1 (4)	1 (2)	<.001
Sputum production				
Morning	22 (23)	2 (8)	2 (4)	.004
All day	4 (4)	0	0	.36
Chronic	1 (1)	0	0	...
Dyspnea (grade 1)	40 (41)	10 (39)	8 (16)	.005
Wheezing	32 (33)	1 (4)	3 (6)	<.001

Note.—Numbers in parentheses are percentages.
* Determined with the Fischer test.

(lobar and segmental) and peripheral (subsegmental and smaller) bronchi was performed. The CT signs were coded as present or absent on the two sets of CT scans obtained.

To determine the distribution of parenchymal abnormalities, the lungs were divided into the following six areas: the upper zones, superior to the level of the carina; the middle zones, between the level of the carina and the level of the inferior pulmonary veins; and the lower zones, inferior to the level of the inferior pulmonary veins. Vertical, anteroposterior, and central-peripheral distribution of parenchymal abnormalities were evaluated on the HRCT scans. The unilateral or bilateral distribution of dependent areas of attenuation was evaluated on conventional CT scans.

Qualitative evaluation of the areas of ground-glass attenuation helped determine the intensity and extent of the areas of increased attenuation. Areas of ground-glass attenuation were classified as (a) homogeneous (involving all the lung with an equal degree and identified by means of the darker air bronchogram sign) or heterogeneous (various degrees of increased attenuation were seen throughout the lung); (b) having low or high attenuation; (c) diffusely distributed or sparing areas of more normal lung (classified as disseminated); and (d) having a segmental, subsegmental, or lobular distribution. The number of pulmonary vascular sections through the areas of high attenuation

were classified as either normal or increased, the latter suggestive of increased lung attenuation secondary to increased capillary blood volume.

The percentage of lung involved with emphysema and areas of ground-glass attenuation on HRCT scans was determined with the same scoring system and was respectively coded as the emphysema score and the ground-glass score. For that purpose, all HRCT scans showing emphysema and areas of ground-glass attenuation were considered. HRCT images were analyzed by using a four-point scale, where 0 = normal, 1 = emphysema or areas of ground-glass attenuation involving less than 25% of the image, 2 = emphysema or areas of ground-glass attenuation involving 25%–50% of the image, 3 = emphysema or areas of ground-glass attenuation involving 50%–75% of the image; and 4 = emphysema or areas of ground-glass attenuation involving more than 75% of the image. The scores of all the HRCT images in a zone (ie, upper, middle, or lower zone) were averaged to obtain a zonal score. The scores of the three zones were summed to give a total score. Scores could range from zero to 12. A consensus score was obtained for each patient.

Statistical analysis was performed with SAS software (Cary, NC) with a Tandon 386/20 microcomputer (Moon Park, Calif). The means, standard deviations, and frequencies were calculated. Comparisons of quantitative data were made with one-way analysis of variance (general linear

model procedure) and Student t tests. Analysis of contingency tables was performed with the χ^2 or Fischer exact test when table cells had expected values of less than five.

RESULTS

Clinical, Functional, and Radiographic Findings

Characteristics of the population are reported in Table 1. Smokers consumed an average of 15 cigarettes a day. The three groups did not significantly differ in age, height, weight, or proportion of men to women. There was a higher percentage of women in each group than there were male smokers. These data reflect the sex ratio in the working population asked to participate in the study.

Table 2 summarizes the clinical data obtained from the questionnaire in the three groups studied. There was a significant correlation between current cigarette consumption and the presence of cough (morning and all-day cough, $P < .001$), morning mucous sputum production ($P = .004$), and wheezing ($P < .001$). There was a significantly higher percentage of dyspnea in smokers and ex-smokers than in nonsmokers ($P = .005$). It is notable that a few of the nonsmokers had clinical symptoms.

Results of pulmonary function tests are summarized in Table 3. An overall normal pulmonary function was observed in the three groups; significantly lower values of FEV_1/FVC, MMEF, MEF 25–15, and MEF 25 were seen in ex-smokers. Smokers had significantly lower values of MEF 25–15 compared with nonsmokers. No radiographic evidence of emphysema or abnormal bronchial wall thickening was found in any of our subjects; the interobserver coefficient of agreement was 95% for emphysema and 92% for abnormal bronchial wall thickening.

CT Findings

HRCT depicted parenchymal abnormalities with a higher frequency than did conventional CT (Table 4). Similar results were observed in the evaluation of abnormal bronchial wall thickening; however, HRCT scans were viewed with a higher window center (−400 HU) than conventional CT studies (−600 HU). Interobserver agreement resulting from separate analysis of conventional CT scans in all three groups was 94% for parenchymal micronodules, 96% for subpleural micronodules, 97% for emphysema, 84% for bronchial wall

thickening, and 100% for both dependent areas of attenuation and septal lines.

Detailed results of HRCT studies are summarized in Table 5. Interobserver agreement resulting from separate analysis of HRCT studies was 100% for dependent areas of attenuation and septal lines for all three groups. For smokers, ex-smokers, and nonsmokers, interobserver agreement was 96%, 100%, and 100%, respectively, for parenchymal micronodules; 92%, 100%, and 100%, respectively, for areas of ground-glass attenuation; 98%, 100%, and 100%, respectively, for emphysema; 93%, 92%, and 100%, respectively, for abnormal bronchial wall thickening; and 96%, 77%, and 96%, respectively, for subpleural micronodules.

Smokers.—HRCT depicted parenchymal micronodules in 26 of the 98 smokers (27%). These nodules were 2–3 mm in diameter, had no definable relation to the secondary pulmonary lobule, and were ill defined, never obscuring adjacent pulmonary vessels (Fig 1). Parenchymal nodules were observed exclusively in the upper lung zones in 19 of the 26 subjects (73%), in the anterior and posterior zones in 21 (81%), and in the central and peripheral zones in 22 (85%).

Areas of ground-glass attenuation were seen in 20 of the 98 smokers (20%) and were observed exclusively in the upper lung zones in 15 subjects (75%) and in the upper, middle, and lower lung zones in five (25%). All areas of ground-glass attenuation were homogeneous and slightly hyperattenuating; normal pulmonary vascular sections were seen through the hyperattenuating area in all subjects. Areas of ground-glass attenuation were diffusely distributed in 15 smokers (75%) and spared some normal lung (ie, disseminated) in five (25%) (Figs 2, 3, 4b). Fourteen subjects had a ground-glass score of 4, three had a score of 3, and three had a score of 2.

Emphysematous changes, detected in 20 of the 98 smokers (20%), were observed exclusively in the upper zones in 13 subjects (65%) and in both the upper and middle zones in seven (35%); the predominance in the upper zone was significant ($P < .01$). Morphologic features of emphysema were as follows: Emphysema was bullous in 14 subjects (70%), nonbullous in 18 (90%), and paraseptal in 15 (75%) and was diversely distributed throughout the lung (Fig 2). Emphysematous changes had a peripheral distribution in 13 subjects (65%), were exclusively seen in the posterior lung

in nine (45%), and were anteriorly and posteriorly situated in 11 (55%). A low total emphysema score was always observed: 17 subjects had an emphysema score of 1, and three had a score of 2.

HRCT depicted abnormal bronchial wall thickening in proximal and peripheral bronchi in 32 smokers (33%) without any other bronchial abnormality (Figs 1, 4b). Dependent areas of attenuation were seen in 33 smokers (34%) and were observed exclusively

in the lower zones in 12 subjects (36%), in the middle and lower zones in 17 (52%), and in the upper, middle, and lower zones in four (12%), but were never exclusively seen in the upper zones. This CT sign was unilateral in eight of the 33 subjects (24%), and was on the right side in seven (21%) and on the left side in one (3%). Dependent areas of attenuation were bilateral in 25 subjects (76%) and were symmetric in 15 (60%) and right-sided in 10 (40%).

Table 3
Results of Pulmonary Function Tests

Parameter	Smokers ($n = 98$)	Ex-smokers ($n = 26$)	Nonsmokers ($n = 51$)	Analysis of Variance
FVC	1.03 ± 0.122	1.01 ± 0.11	1.04 ± 0.155	F = 0.43 (P = .65)
FEV$_1$	1.03 ± 0.130	0.98 ± 0.130	1.05 ± 0.144	F = 2.2 (P = .10)
FEV$_1$/FVC	1.00 ± 0.070	0.97 ± 0.068	1.01 ± 0.064	F = 3.1 (P = .04)
MEF 75–25	1.02 ± 0.282	0.87 ± 0.212	1.04 ± 0.204	F = 4.0 (P = .01)
MEF 25–15	1.05 ± 0.373	0.89 ± 0.298	1.18 ± 0.289	F = 5.7 (P = .004)
MEF	1.12 ± 0.193	1.07 ± 0.192	1.12 ± 0.187	F = 0.7 (P = .47)
MEF 75	1.17 ± 0.253	1.14 ± 0.257	1.15 ± 0.237	F = 0.2 (P = .77)
MEF 50	1.03 ± 0.266	0.92 ± 0.237	1.02 ± 0.215	F = 2.0 (P = .13)
MEF 25	0.93 ± 0.314	0.79 ± 0.295	1.03 ± 0.305	F = 5.2 (P = .006)
MEF 50/MEF	0.55 ± 0.127	0.51 ± 0.131	0.56 ± 0.132	F = 0.9 (P = .37)

Note.—Test results are expressed as measured to predicted ratios and are presented as mean ± standard deviation. Despite some statistically significant differences between groups, the results are within the normal range, thus excluding presence of small-airways disease in the population studied.

Table 4
Detection of Bronchopulmonary Abnormalities with Conventional CT and HRCT

Finding	Conventional CT ($n = 175$)	HRCT ($n = 175$)	P Value*
Micronodules			
Parenchymal	5 (3)	27 (15)	.01
Subpleural	16 (9)	58 (33)	.001
Areas of ground-glass attenuation	...	21 (12)	...
Emphysema	15 (9)	22 (12)	<.001
Bronchial wall thickening	17 (10)	45 (26)	<.001
Dependent areas of attenuation	50 (29)	50 (29)	...
Septal lines	0	12 (7)	<.01

Note.—Numbers in parentheses are percentages.
* Determined with the Fischer test.

Table 5
HRCT Findings

Finding	Smokers ($n = 98$)	Ex-smokers ($n = 26$)	Nonsmokers ($n = 51$)	P Value
Parenchymal micronodules	26 (27)	1 (4)	0	<.001
Areas of ground-glass attenuation	20 (21)	1 (4)	0	.001
Emphysema	20 (21)	2 (8)	0	<.001
Bronchial wall thickening	32 (33)	4 (16)	9 (18)	.06
Dependent areas of attenuation	33 (34)	11 (43)	6 (12)	.003
Septal lines	6 (6)	2 (8)	4 (8)	...
Subpleural micronodules	37 (38)	10 (39)	11 (22)	.11

Note.—Numbers in parentheses are percentages.

Subpleural micronodules were observed in 37 smokers (38%), were always of low profusion (less than five micronodules), and were situated posteriorly in 35 subjects (95%) and superiorly in 31 (84%) (Fig 1c).

Forty-six subjects had parenchymal micronodules or areas of ground-glass attenuation. In 29 subjects (63%), those abnormalities were seen in areas with no detectable emphysematous changes; abnormal bronchial wall thickening was detected in five of those 29 subjects.
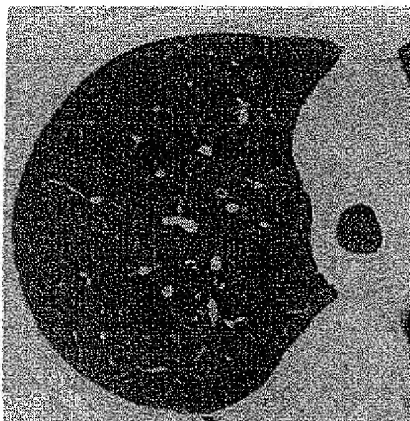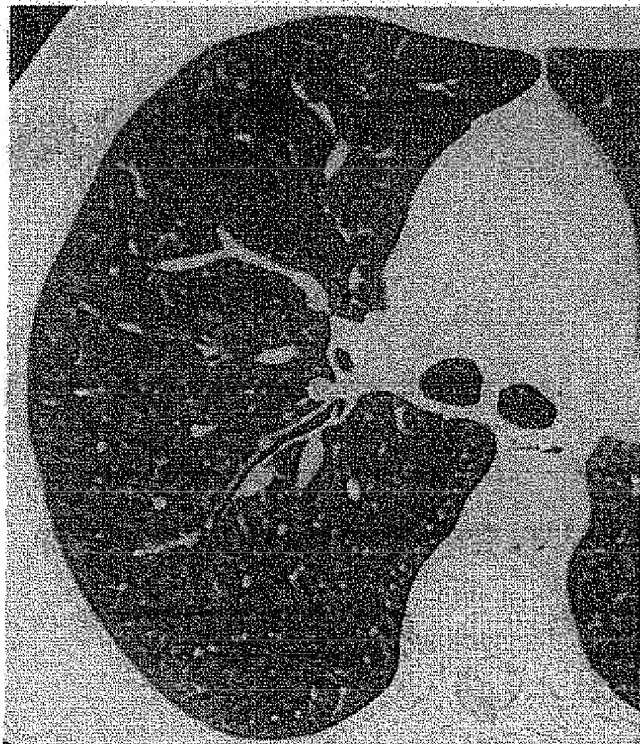
Ex-smokers.—Parenchymal micronodules were observed in only one of the 26 ex-smokers (4%), with the same pattern at HRCT as that observed in smokers. Parenchymal micronodules were seen exclusively in the upper lung zones and were diffusely distributed in the transverse plane. Areas of ground-glass attenuation were seen in one subject (4%). These areas were located exclusively in the upper lung zone, were of low attenuation, and were diffusely distributed. The increased lung attenuation was homogeneous, and vascular sections were normal; the total ground-glass score was 2. Areas of ground-glass attenuation and micronodules were not seen in the same subject.

Emphysema was detected in two of the 26 ex-smokers (8%) and was observed exclusively in the upper lung zones, was paraseptal and bullous, and involved the posterior part of the lung. Both subjects had a total emphysema score of 1. Four subjects (15%) were considered to have abnormal bronchial wall thickening, of both central and peripheral bronchi, without any other bronchial abnormality. Dependent areas of attenuation were observed in 11 ex-smokers (42%) and were seen exclusively in the lower zones in nine (82%) and in the middle and lower zones in two (18%). These dependent areas of attenuation were unilateral in six subjects (55%) (right-sided in five, left-sided in one) and bilateral in five (45%). When bilateral, these areas always had a symmetric distribution.

Subpleural micronodules were observed in 10 ex-smokers (38%) and were always of low profusion (less

Figure 1. Parenchymal micronodular patterns in smoker's lung. (a) HRCT scan at the level of the right upper lobe in a 34-year-old smoker shows faint parenchymal micronodules in the central and peripheral parts of the lung. This appearance is clearly different from that of the trachea, which represents image noise. Mild bronchial wall thickening on the peripheral bronchi and a subpleural, posteriorly situated micronodule (arrow) are also seen. (b) HRCT scan at the level of the right upper lobe in a 29-year-old smoker. Small ill-defined micronodules are visible in the axillary area and the posterior segment, sparing the anterior lung and different from image noise observed in right and left main bronchi. (c) HRCT scan at the level of the right lower lobe in a 33-year-old smoker shows small nodular areas of increased attenuation (arrows) diffusely distributed throughout the lower lobe. Adjacent vessels are visualized. Note dependent areas of attenuation and mild peripheral bronchial wall thickening.
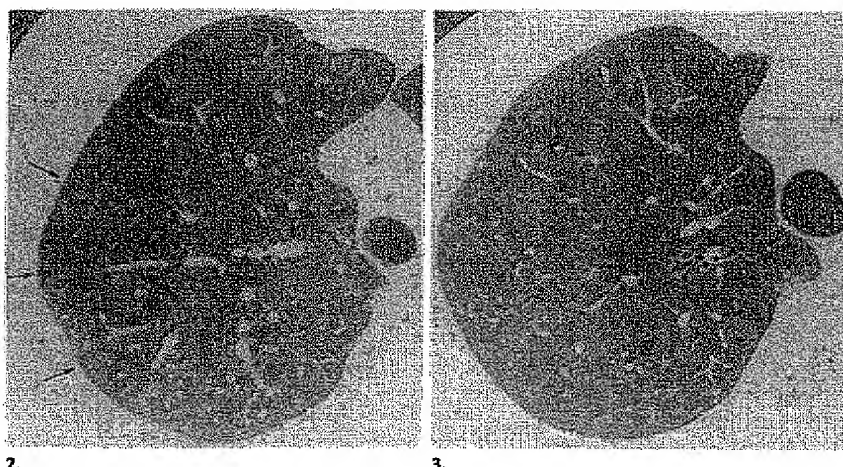
than five micronodules). These micronodules were posteriorly situated in nine subjects (90%) and superiorly situated in eight (80%).

Nonsmokers.—CT did not depict parenchymal micronodules, areas of ground-glass attenuation, or emphysema in any nonsmokers. However, we observed abnormal bronchial wall thickening in nine subjects (18%) (exclusively in central bronchi and without any other bronchial abnormality). Dependent areas of attenuation were seen in six subjects (12%) and were unilateral in five (83%) (right-sided in three, left-sided in two) and bilateral (with a symmetric distribution) in one (17%). Subpleural micronodules were observed in 11 nonsmokers (22%), were always of low profusion (less than five micronodules), and were posteriorly and superiorly situated. Fine, nondistorted septal lines were observed in the center of both lower lobes, with almost the same frequency as that seen in the other two groups studied.

To evaluate the importance of lesions detected with CT in the three groups studied, CT scans were separated into four categories: category 0 = normal, and categories 1, 2, and 3 = one, two, and at least three CT abnormalities, respectively. Detailed results on the distribution of abnormal CT findings among the population studied are summarized in Figure 5a. Among nonsmokers, CT scans were normal in 29 of the 51 subjects (57%) and abnormal in 22 (43%). Four abnormalities, diversely distributed, were seen on CT scans in nonsmokers: subpleural micronodules, bronchial wall thickening, dependent areas of attenuation, and septal lines.

Eighteen of the 98 smokers (18%) had normal CT scans (category 0), whereas 80 smokers (82%) had category 3 scans. There was a significant difference in cigarette consumption between smokers with category 0 scans and those with category 3 scans (eight and 13 pack-years, respectively; $P < .05$). It is notable that parenchymal micronodules and areas of ground-glass attenuation were the two CT findings that enabled differentiation of the three groups. Frequency of the CT signs detectable in smokers according to CT categories are summarized in Figure 5b. When emphysematous changes were detected at CT in smokers or ex-smokers ($n = 22$), it was an isolated finding in two subjects (9%) and was associated with one or more of the following abnormalities in 20 (91%): parenchymal micronodules (35%), subpleural

micronodules (35%), bronchial wall thickening (40%), dependent infiltrates (45%), and nondependent areas of ground-glass attenuation (45%).

Clinical, Functional, and CT Correlations

The following parameters were significantly correlated for all three groups: (a) early morning cough with emphysema ($P = .003$) and bronchial wall thickening ($P = .001$), (b) all-day cough with bronchial wall thickening ($P = .005$), (c) early-day sputum production with emphysema ($P = .05$) and bronchial wall thickening ($P = .001$), (d) dyspnea with emphysema ($P = .02$) and bronchial wall thickening ($P = .009$), and (e) wheezing with parenchymal micronodules ($P < .001$), emphysema ($P = .002$), and bronchial wall thickening ($P < .001$).

Of the abnormal CT findings in the three groups studied, emphysema and abnormal bronchial wall thickening were the only CT signs observed with significantly lower functional parameters. Patients with emphysema had significantly lower values for FEV_1/FVC ($t = 1.94$, $P = .005$) and MEF 75 ($t = 2.44$, $P = .001$). The presence of central or peripheral bronchial wall thickening was observed with significantly lower values of MEF 75 ($t = 2.90$, $P = .004$) and MEF 50 ($t = 2.02$, $P = .04$). Dependent areas of attenuation were observed with higher frequency in current and ex-smokers than in nonsmokers; however, no correlation was found be-

tween this CT sign and abnormal pulmonary function, especially with functional parameters evaluating small-airways obstruction.

DISCUSSION

In our study, we excluded smokers with physician-diagnosed respiratory disease or previous history of respiratory bronchiolitis of any cause; all of our subjects perceived themselves to be healthy. Despite this perceived good health, however, a few subjects had mild symptoms of simple chronic bronchitis, commonly considered by smokers as "normal" symptoms, although their pulmonary functions were normal. However, single-breath nitrogen washout and closing capacity tests, which are sensitive for early detection of small-airways disease, were not performed in our study (19).

If inflammation in the airways is present in most smokers, it has been speculated that clinically important airways obstruction will develop only in those in whom the inflammatory response is associated with excessive connective tissue deposition, often observed in heavy smokers (1,4–6). Absence of functional impairment in our study population, comprising healthy, middle-aged smokers, is consistent with physiologic studies in young smokers whose spirometric values are unchanged or only minimally altered (1,20,21). Jaakkola et al (20) have recently observed that cigarette smoking has a dose-related adverse effect on the evolution of the

Figures 2, 3.   (2) HRCT scan at the level of the right upper lobe in a 25-year-old smoker shows areas of ground-glass attenuation diffusely distributed through the lung and responsible for the darker air bronchogram sign. Note the small emphysematous areas in the subpleural axillary region (arrows) and the central part of the lung (arrowheads). (3) HRCT scan at the level of the right upper lobe in a 31-year-old smoker demonstrates multifocal or disseminated distribution of areas of ground-glass attenuation alternating with more normal lung.

Figure 4. Abnormal bronchial wall thickness. (a) HRCT scan at the level of the inferior pulmonary vein in a 35-year-old asymptomatic non-smoker shows normal central and peripheral bronchi with thin, sharply defined walls and normal lung attenuation. (b) HRCT scan at the level of the right inferior pulmonary vein in a 29-year-old smoker shows marked abnormal bronchial wall thickening in the central and peripheral bronchi. Presence of a darker air bronchogram in the middle and lower lobes helps recognize areas of ground-glass attenuation. Note the mild interlobular septal thickening in the medial segment of the middle lobe (arrows).
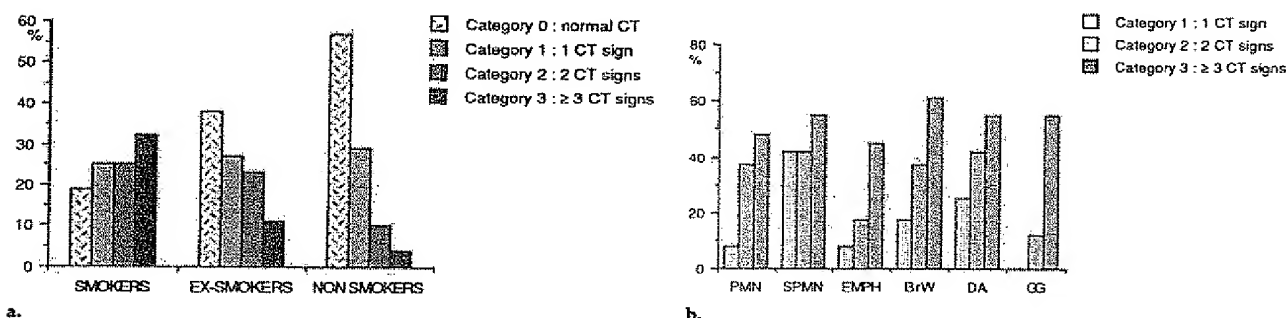
Figure 5. (a) Relationship between lung abnormalities detected with HRCT and smoking habits. The relationship was statistically significant ($P < .001$). (b) Frequency of abnormalities in smokers according to CT category. PMN = parenchymal micronodules, $SPMN$ = subpleural micronodules, $EMPH$ = emphysema, BrW = bronchial wall thickening, DA = dependent areas of attenuation, GG = areas of ground-glass attenuation.

ventilatory lung function in young adults. These data explain why the idea that pulmonary function tests enable detection of "early" and potentially reversible lung disease is controversial and that the need for a sensitive means of early detection of chronic obstructive pulmonary disease is still present (5,7,22).

Pathologic similarities of bronchiolitis resulting from environmental insult (23) and cigarette smoking (1–3) have led us to postulate that small to medium-size lesions in smokers could be detected with CT as parenchymal micronodules. In our study, we observed small parenchymal micronodules of low attenuation in 27% of cur-

rent smokers, with an exclusive distribution in the upper lung zones in 71% of cases. These micronodules were seen in a few ex-smokers but were never seen in nonsmokers, suggesting a possible relationship with smoker's bronchiolitis in the absence of any history of respiratory illness or occupational or environmental expo-

sure to pollutants in the population studied.

HRCT depicted abnormalities as small nodular areas of increased attenuation, with ill-defined borders, scattered throughout the lung parenchyma. These abnormalities had no definable distribution within the secondary pulmonary lobule and were sometimes difficult to differentiate from heterogeneous areas of ground-glass attenuation. Reliable detectability of these subtle abnormalities is closely related to a cautious interpretation of HRCT images because of the well-known impact of window width and level on the appearance of the lung parenchyma and the dimensions of visualized structures. Care must be taken to avoid low window settings with narrow window widths, which leads to preferential magnification of small structures and, thus, spuriously creates a false impression of a micronodular pattern. The lesions observed in smoker's lung can be diagnosed only with a correct choice of the window settings used for photography of HRCT images, that is, a large window width (range, 1,500–2,000 HU) and high window level (range, −500 to −700 HU).

We believed that we could detect macrophage alveolitis, a constant finding at bronchoalveolar lavage or pathologic examination of a specimen from a smoker's lung, with CT as areas of ground-glass attenuation. Because areas of ground-glass attenuation have been described in association with various inflammatory processes involving the alveolar spaces and/or the interstitium of patients with chronic diffuse infiltrative lung disease, we expected to find them in smokers' lungs on HRCT images (24).

Areas of ground-glass attenuation were observed in 21% of smokers and in only one ex-smoker but were never detected in nonsmokers. Areas of ground-glass attenuation consisted of areas of increased lung density, were always homogeneous, and were slightly hyperattenuating. Areas of ground-glass attenuation were diffusely distributed in 75% of the subjects and spared some normal lung in the remaining 25%. In cases of mild and heterogeneously distributed gradients of attenuation in the lung parenchyma, it was sometimes difficult to distinguish a pattern of normal lung with areas of ground-glass attenuation from that of areas of abnormally low attenuation with normal lung. If increased lung attenuation is related to increased cellularity within alveoli in smokers, its pattern may

also reflect areas of disparate lung perfusion resulting from air trapping in patients with bronchiolitis, especially when disseminated. Increased regional differences in lung attenuation on expiratory scans would have supported our hypothesis, but additional expiratory scans were not systematically included in our protocol.

We never observed large pulmonary vascular sections within areas of increased lung attenuation. Increased diameter of pulmonary vessels is a useful CT indicator of areas of ground-glass attenuation related to redistribution of blood flow in pulmonary diseases, but it may vary according to the severity and extent of the underlying pulmonary process (24). Optimal assessment of areas of ground-glass attenuation also requires awareness of the influence of window settings on the appearance of pulmonary structures and analysis of lung attenuation; the use of low window settings can cause a so-called ground-glass appearance. Despite the subjectivity of the visual assessment of mild parenchymal changes, such as areas of ground-glass attenuation and micronodules, the high interobserver agreement in our study indicates that these subtle findings can be reliably detected on HRCT scans.

Many investigators have evaluated the role of smoking in the pathogenesis of emphysema, but, to our knowledge, there have been few reports concerning the evaluation of the emphysematous changes in smokers. As previously reported (10,25–27), HRCT is the most sensitive method available for detection of mild emphysema. In our study, HRCT enabled us to make a definitive diagnosis of emphysema in smokers and ex-smokers despite nondiagnostic radiographic and pulmonary function test findings. However, we performed only a limited evaluation of pulmonary function because of the limitations in the material used, thus precluding measurement of diffusing capacity, known as a sensitive indicator for emphysema (27). The low frequency of emphysema in our population has to be interpreted in light of the report by Auerbach et al (28), who demonstrated that, among subjects who continue to smoke, the degree of disease increased with age.

The transverse distribution of emphysematous changes observed in our study are consistent with the observation that centrilobular emphysema is often distributed irregularly or in a patchy fashion within the lungs (29,30). Moreover, the upper

lobe predominance of emphysema on HRCT scans confirms well-established pathologic data (31–33). A striking finding in our study was that parenchymal micronodules, areas of ground-glass attenuation, and emphysema were observed with a similar predominance in the upper lung zones, suggesting that these morphologic changes were induced by cigarette smoke. Moreover, these CT findings also support previously reported data suggesting a causal association between small-airways disease and emphysema (3,7). It is assumed that the inflammatory process is a precursor of the destructive changes that occur in the bronchioles, thus resulting in centroacinar emphysema (1,3).

Analysis of the bronchial wall is markedly influenced by the choice of window settings; however, the CT numbers used in our study enabled us to exclude falsely prominent bronchial walls, a feature commonly seen when low window settings are used. However, the position of the window center has an important effect on the apparent dimensions of structures on the CT image (34). In our study, variation in the window centers selected for conventional CT (−400 HU) and HRCT (−600 HU) could explain the differences observed between the two CT techniques in the detection of bronchial wall thickening. On HRCT scans, abnormal bronchial wall thickening of central and peripheral bronchi was observed with a significantly higher frequency in smokers; this finding was also observed in ex-smokers with mild clinical symptoms and in a few asymptomatic nonsmokers. Because our study was based on a visual and, thus, subjective analysis of bronchial wall thickness, we cannot exclude an overrecognition of mild bronchial abnormalities. However, the CT findings have to be interpreted in the context of clinical data, and the presence of mild respiratory symptoms in nonsmokers suggests the presence of actual bronchial irritation in this group.

It is well known that small-airways responses to cigarette smoke are not specific and that other causes for small-airways disease may exist (1,7). In the absence of asthma, occupational exposure to pollutants, or other environmental conditions, the contribution of air pollution to the development of chronic bronchitis in our population of urban dwellers may be questioned. Because cigarette smoking is a well-known cause of simple anthracosis located subpleurally, the presence of subpleural micronodules

in healthy adult smokers is not surprising. The low profusion of these micronodules, their predominant distribution in the posterior and superior subpleural areas, and the absence of confluence in large pseudoplaques are the most useful features to differentiate them from subpleural micronodules that occur in chronic diffuse interstitial lung disease (35). However, subpleural micronodules were detected in 22% of our nonsmokers, which may be suggestive of the influence of urban living, another common cause of simple anthracosis located interstitially and subpleurally.

Despite the absence of a pathologic substratum in our population, the CT findings observed suggest that HRCT can help identify mild parenchymal abnormalities in smokers with normal pulmonary function who present with minimal or no clinical symptoms. These data confirm that, except in severe cases of widespread and extensive emphysema, which are accurately depicted on chest radiographs, chest radiography cannot routinely depict the presence of mild disease (29,36,37). This raises the possibility that early detection of parenchymal abnormalities on HRCT scans, after cessation of smoking, may help prevent the development of disabling obstructive airflow disease known to develop in a minority of ex-smokers (21,38). Because our investigation was a cross-sectional study, further longitudinal follow-up is mandatory to evaluate bronchial, bronchiolar, and parenchymal changes over the years. Moreover, this study may help clarify the contentious role of cigarettes in the development of radiographically detectable opacities in populations with occupational exposure to airborne agents and may help detect respiratory illness in passive smokers. ▨

References

1. Niewoehner DE, Kleinerman J, Rice DB. Pathologic changes in the peripheral airways of young cigarette smokers. N Engl J Med 1974; 291:755–758.
2. Cosio M, Gezzo H, Hogg JC, et al. The relations between structural changes in small airways and pulmonary function tests. N Engl J Med 1977; 298:1277–1281.
3. Willems LNA, Kramps JA, Stijnen T, Sterk PJ, Weening JJ, Dijkman JH. Relation between small airways disease and parenchymal destruction in surgical lung specimens. Thorax 1990; 45:89–94.
4. Wright JL, Lawson LM, Pare PD, Kennedy S, Wiggs B, Hogg JC. The detection of small airways disease. Am Rev Respir Dis 1984; 129: 989–994.
5. Bosken CH, Wiggs BR, Pare PD, Hogg JC. Small airway dimensions in smokers with obstruction to airflow. Am Rev Respir Dis 1990; 142:563–570.
6. Adesina AM, Vallyathan V, McQuillen EN, Weaver SO, Craighead JE. Bronchiolar inflammation and fibrosis associated with smoking: a morphologic cross-sectional population analysis. Am Rev Respir Dis 1991; 143:144–149.
7. Cosio MG, Hale KA, Niewoehner DE. Morphologic and morphometric effects of prolonged cigarette smoking on the small airways. Am Rev Respir Dis 1980; 122:265–271.
8. Demedts M, Aumann JF. Early emphysema: ten years' evolution. Chest 1988; 94:337–342.
9. Bergin CJ, Muller NL, Miller RR. CT in the quantitative assessment of emphysema. J Thorac Imaging 1986; 1:94–103.
10. Kuwano K, Matsuba K, Ikeda T, et al. The diagnosis of mild emphysema: correlations of computed tomography and pathologic scores. Am Rev Respir Dis 1990; 141:169–178.
11. British Occupational Hygiene Society Committee on Hygiene Standards. A basis for hygiene standards for flax dusts. Ann Occup Hyg 1980; 23:1–26.
12. American Thoracic Society. Definition and classification of chronic bronchitis, asthma and pulmonary emphysema: a statement by the Committee on Diagnostic Standard for Non-Tuberculous Respiratory Diseases. Am Rev Respir Dis 1962; 85:762.
13. American Thoracic Society. Snowbird workshop on standardization of spirometry. Am Rev Respir Dis 1979; 119:831–838.
14. American Thoracic Society. Standardization of spirometry: update. Am Rev Respir Dis 1987; 136:1285–1298.
15. Knudson RJ, Slatin RC, Lebowitz MD, Burrows B. The maximal expiratory flow volume curve: normal standards, variability and effects of age. Am Rev Respir Dis 1976; 113:587–600.
16. Knudson RJ, Lebowitz MD, Holberg CJ, Burrows B. Changes in the normal expiratory flow volume curve with growth and aging. Am Rev Respir Dis 1983; 127:725–734.
17. Morris JF. Spirometry in the evaluation of pulmonary function: medical progress. West J Med 1976; 125:109–118.
18. Remy-Jardin M, Remy J, Deffontaines C, Duhamel A. Assessment of diffuse infiltrative lung disease: comparison of conventional CT and high-resolution CT. Radiology 1991; 181: 157–162.
19. Wright JL, Churg A. Cigarette smoke causes physiologic and morphologic changes of emphysema in the guinea pig. Am Rev Respir Dis 1990; 142:1422–1428.
20. Jaakkola MS, Ersnt P, Jaakkola JJK, N'gan'ga LW, Becklake MR. Effect of cigarette smoking on evolution of ventilatory function in young adults: an eight-year longitudinal study. Thorax 1991; 46:907–913.
21. Knudson RJ, Knudson DE, Kaltenborn WT, Bloom JW. Subclinical effects of cigarette smoking: a five-year follow-up of physiologic comparisons of healthy middle-aged smokers and nonsmokers. Chest 1989; 95:512–518.
22. Niewhoener DE, Kleinermen J. Morphologic basis of pulmonary resistance in the human lung and effect of aging. J Appl Physiol 1974; 36:412–418.
23. Wright JL, Churg A. Morphology of small airway lesions in patients with asbestos exposure. Hum Pathol 1984; 15:68–74.
24. Remy-Jardin M, Remy J, Giraud F, Wattinne L, Gosselin B. Computed tomography (CT) assessment of ground glass opacity: semiology and significance. J Thorac Imaging (in press).
25. Bergin C, Muller NL, Nichols DM, et al. The diagnosis of emphysema: a computed tomographic–pathologic correlation. Am Rev Respir Dis 1986; 133:541–546.
26. Sanders C, Nath H, Bailey WC. Detection of emphysema with computed tomography: correlation with pulmonary function tests and chest radiography. Invest Radiol 1988; 23:262–266.
27. Klein JS, Gamsu G, Webb WR, Golden JA, Muller NL. High-resolution CT diagnosis of emphysema in symptomatic patients with normal chest radiographs and isolated low diffusing capacity. Radiology 1992; 182:817–821.
28. Auerbach O, Hammond EC, Garfinkel L, Benante C. Relationship of smoking and age to emphysema: whole-lung section study. N Engl J Med 1972; 286:853–857.
29. Thurlbeck WM, Henderson JA, Fraser RG, Bates DV. Chronic obstructive lung disease. Medicine 1970; 49:81–145.
30. Wyatt JP, Fischer VW, Sweet HC. The pathomorphology of emphysema complex. I. Am Rev Respir Dis 1964; 89:533–560.
31. Berend N, Skoog C, Thurlbeck WM. Lobar pressure-volume characteristics of excised human lungs. Thorax 1981; 36:290–295.
32. Cockroft DW, Horne SL. Localization of emphysema within the lung: hypothesis based upon ventilation/perfusion relationships. Chest 1982; 82:483–487.
33. Wright JL, Wiggs BJ, Hogg JC. Airway disease in upper and lower lobes in lungs of patients with and without emphysema. Thorax 1984; 39:282–285.
34. Koehler PR, Anderson RE, Baxter B. The effect of computed tomography viewer controls on anatomical measurements. Radiology 1979; 130:189–194.
35. Remy-Jardin M, Beuscart R, Sault MC, Marquette CH, Remy J. Subpleural micronodules in diffuse infiltrative lung diseases: evaluation with thin-section CT scans. Radiology 1990; 177:133–139.
36. Milne ENC, Bass H. The roentgenographic diagnosis of early chronic obstructive pulmonary disease. J Can Assoc Radiol 1969; 20:3–15.
37. Woodring JH, Philips BA, West J, Ulmer J, Cooper JK. A prospective evaluation of plain radiographic signs of chronic obstructive pulmonary disease. J Thorac Imaging 1991; 6:14–21.
38. Rennard SI, Daughton D, Fujita J, et al. Short-term smoking reduction is associated with reduction in measures of lower tract inflammation in heavy smokers. Eur Respir J 1990; 3:752–759.